



CDF/PUB/EXOTIC/PUBLIC/10065

Search for a SM Higgs Boson with the Diphoton Final State at CDF

The CDF Collaboration

URL <http://www-cdf.fnal.gov>

(Dated: February 23, 2010)

Abstract

A search for the Higgs boson in the diphoton decay channel is reported. Although the Standard Model branching fraction is small, the diphoton final state is appealing due to better diphoton mass resolution compared with dijet final states. In addition, other models — such as fermiophobic models where the Higgs does not couple to fermions — predict much larger branching fractions for the diphoton decay. Here, for the first time, we search diphoton data from the CDF experiment for signs of a standard model Higgs boson.

Preliminary Results

I. INTRODUCTION

Low mass Higgs boson searches at the Tevatron usually focus on the dominant $b\bar{b}$ decay channel. The diphoton final state is appealing because the photon ID efficiency and energy resolution are much better than that of b -jets. The photon's better energy resolution leads to a narrow $M_{\gamma\gamma}$ mass peak which can be exploited to reduce backgrounds. In the standard model (SM), however, the branching fraction for the diphoton ($\gamma\gamma$) final state $B(h \rightarrow \gamma\gamma)$ has a maximal value of approximately 0.2% for Higgs masses of about 120 GeV/c². Nevertheless, it is interesting to make a statement on the sensitivity of the CDF experiment to the SM $h \rightarrow \gamma\gamma$ process.

In addition to SM $h \rightarrow \gamma\gamma$ production, one can devise many possible Beyond the Standard Model (BSM) scenarios where $B(h \rightarrow \gamma\gamma)$ is enhanced. An informative summary of the various models that modify $B(h \rightarrow \gamma\gamma)$ can be found in Reference [1]. The “fermiophobic” Higgs (h_f) benchmark model assumes SM coupling to bosons and vanishing couplings to all fermions. The higher branching fraction causes a larger number of potential fermiophobic Higgs events compared to that predicted by the SM. Any resonance observed could also then be evidence for a BSM Higgs.

In the past, there have been phenomenological discussions of searches for h_f at the Tevatron experiments [2], as well as experimental searches at LEP [3]. In Run I, CDF searched for the fermiophobic Higgs [4] and recently for Run II, DØ published a paper [5] focusing on the same search. Most recently, CDF published a search for h_f with $\sim 3 \text{ fb}^{-1}$ [6] and DØ published a search for the SM Higgs with $\sim 3 \text{ fb}^{-1}$ [7].

For this study, we focus on the sensitivity of a CDF search for SM $h \rightarrow \gamma\gamma$. All cross sections are calculated by HIGLU and branching fractions are calculated by HDECAY [8]. These values are summarized in Table I.

II. DATA SET, EVENT SELECTION, AND PHOTON ID

This analysis uses data between February 2004 and July 2009 and comprises approximately 5.4 fb^{-1} of integrated luminosity. Signal Monte Carlo was generated using PYTHIA 6.2 [9] using CTEQ5 [10] parton distribution functions, and the standard CDF underlying event tune [11].

M_h (GeV/c ²)	$\sigma(g \text{ fusion})$ pb	$\sigma(W_{\text{associated}})$ pb	$\sigma(Z_{\text{associated}})$ pb	$\sigma(VBF)$ pb	$B(h \rightarrow \gamma\gamma)$
100	1.9	0.29	0.17	0.010	0.0015
110	1.4	0.21	0.12	0.087	0.0019
120	1.1	0.15	0.093	0.072	0.0022
130	0.86	0.11	0.071	0.063	0.0022
140	0.68	0.086	0.054	0.053	0.0019
150	0.55	0.066	0.043	0.46	0.0014

TABLE I: Cross sections for SM Higgs production and branching fractions for SM Higgs decays.

The diphoton triggers, base event selection, and photon identification requirements are exactly the same as the recently published high-mass search for Randall-Sundrum gravitons decaying to the $\gamma\gamma$ final state (see References [12]) and therefore will not be discussed in detail here.

All events are required to have at least one reconstructed event vertex. The primary vertex of an event is additionally required to be in the region of the detector consistent with $p\bar{p}$ beam-beam interaction. Only events which include two central photons with $|\eta| < 1.05$ (CC) are selected. Photon ID efficiencies were studied using electrons from Z boson decays and differences between detector response and CDF simulation of the detector were also corrected based on these studies.

III. THE CDF DETECTOR

The CDF detector is described in many available references [13, 14].

IV. DETECTOR ACCEPTANCE AND ID EFFICIENCIES

The detector acceptance was studied using PYTHIA Monte Carlo production events passed through a simulation for the CDF detector, CDFSIM, based on GEANT [15] and GFLASH [16]. The remaining events that additionally passed the same photon ID selection as the data, were then used to obtain an overall signal acceptance for each signal process and mass point. These values are given in Table II.

Acceptance (%)			
M_h (GeV/c ²)	g fusion	$h + W/Z$	VBF
100	11.6	12.3	13.2
110	11.8	12.7	13.7
120	12.3	13.2	14.1
130	12.8	13.4	14.2
140	13.1	13.9	14.7
150	13.7	14.1	15.1

TABLE II: Central signal acceptance, in percent, for each production process and mass point generated.

V. BACKGROUND MODEL

The width of the $M_{\gamma\gamma}$ signal peak (shown in Figure 1) is on the order of a few GeV/c² and is only limited by detector resolution. This means that we are searching for a very narrow peak on the smooth background distribution (Figure 2) composed of both SM diphoton events and events in which one or two jets fake a photon. Modeling of this background combination is possible, but non-trivial, and is not necessary for dedicated searches for a narrow mass peak. Therefore, rather than model each background component directly, this analysis assumes a null hypothesis – after visual confirmation that no obvious peak exists in the data, a smooth curve is fit to the data. This fit first excludes a 12 GeV window around each mass point and is then interpolated to the signal region. The fit in the signal region serves as the background model for predicting the expected sensitivity and for testing against the data for the signal hypothesis at the various mass points.

An example fit obtained from a mass window around 120 GeV/c² is shown in Figure 3, along with the corresponding residual plot of (data – fit)/(stat error). A rate systematic is derived based on the uncertainty of the fit in the signal region. A value of 4% was obtained and is included when setting limits.

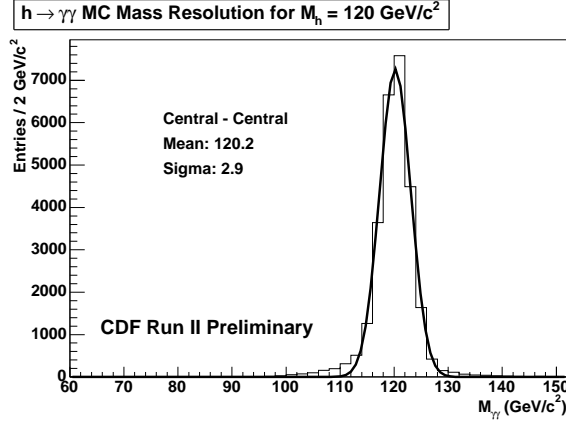


FIG. 1: $M_{\gamma\gamma}$ mass peak for $M_h = 120 \text{ GeV}/c^2$ with a Gaussian width σ less than $3 \text{ GeV}/c^2$.

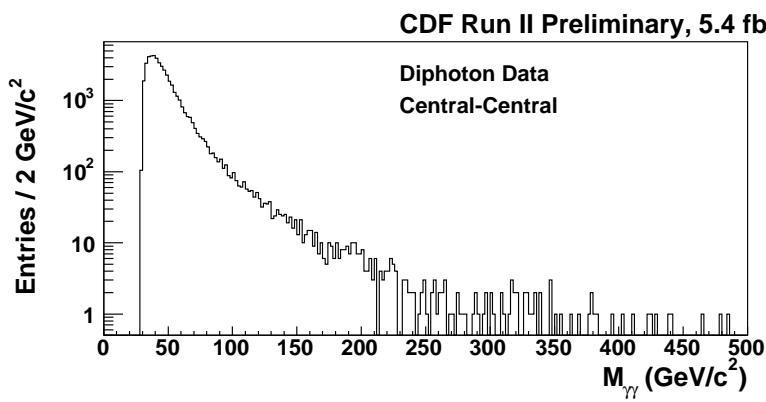


FIG. 2: $M_{\gamma\gamma}$ for central-central photons.

VI. SYSTEMATIC UNCERTAINTIES

Systematic uncertainties on signal MC shapes include uncertainties in the production cross section, the integrated luminosity, and on the acceptance and efficiency. A 6% uncertainty on the integrated luminosity considers uncertainty in $p\bar{p}$ inelastic cross section and acceptance of CDF's luminosity monitor. The theoretical uncertainties on the production cross sections used are 12% for gluon fusion, 5% for associative production Higgs production with a W or Z , and 10% for vector boson fusion. All systematics on acceptance and efficiency are shown in Table III and described below.

The PDF uncertainty on event acceptance was calculated using the CTEQ61.M [17, 18] error sets and a standard event re-weighting technique [19, 20]. ISR and FSR uncertainties were studied using MC samples with modified parton shower parameters. The energy scale

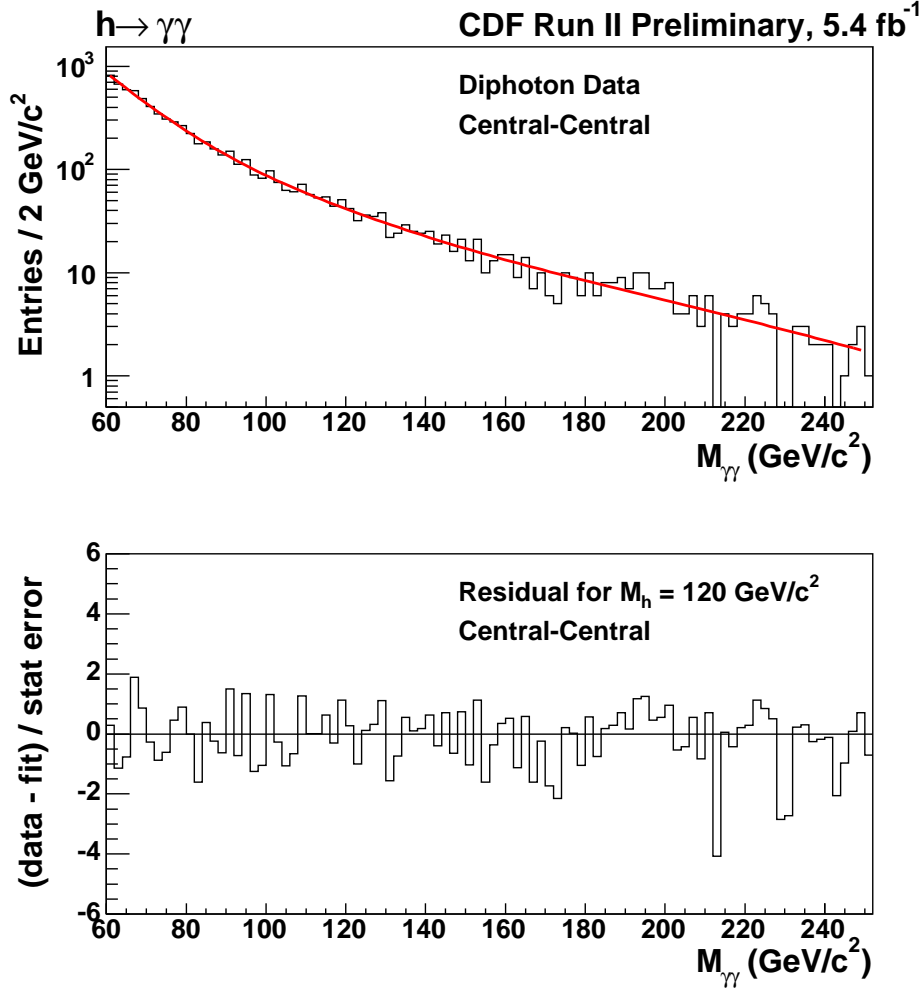


FIG. 3: Smooth fits to central diphoton data with the SM Higgs event selection. The example fit shown was obtained by first excluding a $12 \text{ GeV}/c^2$ window around a signal mass of $M_h = 120 \text{ GeV}/c^2$ and then interpolating into this region. The fit in the signal region serves as the null hypothesis background model. The data vs. fit residual is also shown.

systematic uncertainty of the CEM was studied by checking the effect on the acceptance of varying the CEM scale by 1%.

The vertex systematic takes into account the efficiency of reconstructing vertices in an event. Since events are required to lie in the region of the detector consistent with $p\bar{p}$ interactions, the vertex systematic additionally takes into account the fraction of collisions that do not. The uncertainty on efficiency from removing $\gamma \rightarrow e^+e^-$ conversions is due to the uncertainty on material included in the simulation of the CDF detector. Photon ID efficiencies were studied using electrons from Z boson decays. There are small differences,

Systematic Errors (%) on signal MC	
Luminosity	6
σ_{ggH} / σ_{VH} / σ_{VBF}	12 / 5 / 10
PDF	1
ISR	2
FSR	2
Energy Scale	0.1
Vertex	0.2
Conversions	0.2
Photon/Electron ID	1.0
Run Dependence	1.5
Data/MC fits	0.2

TABLE III: Summary of systematic errors applied to signal MC.

however, in the shower profiles of electrons and photons which may affect these studies. To account for this, a systematic was taken based on the difference between photon and electron efficiencies observed in the MC with detector simulation. A single data-MC scale factor is applied to the full MC sample, however, the variations of this factor between data taking periods was included as a systematic. Finally, the uncertainties on the fits used to study ID efficiencies are propagated as uncertainty.

A 4% rate uncertainty is applied to the background shape as described in the previous section.

VII. RESULTS

The theoretical production cross section and branching fraction were given in Table I [8] and detector acceptance for each mass point is in Table II. These values, as well as the invariant mass distributions for the signal and background model, are used to set limits on $h \rightarrow \gamma\gamma$ production. Only the 12 GeV/ c^2 signal region of the $M_{\gamma\gamma}$ distributions is used in obtaining these limits.

M_h (GeV/ c^2)	Expected Limit	Observed Limit
100	25.7	24.3
110	21.5	25.9
120	19.4	22.5
130	20.6	18.7
140	25.5	32.9
150	38.6	40.0

TABLE IV: Expected and observed limits relative to the SM prediction obtained from central photons.

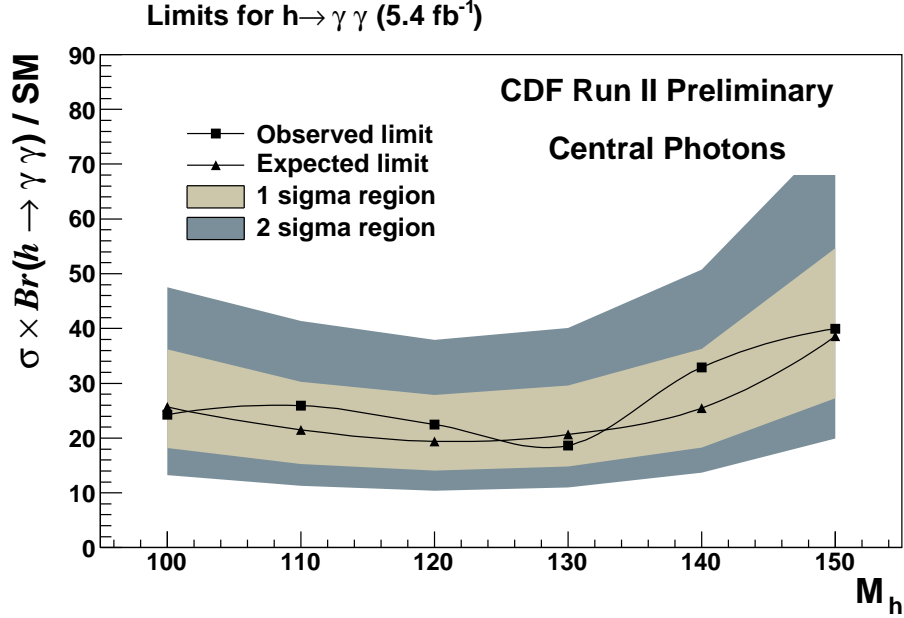


FIG. 4: Cross section times branching fraction limits relative to the SM as a function of Higgs mass.

A binned-likelihood method is applied using Poisson fluctuations of the $M_{\gamma\gamma}$ bin contents in order to set limits on sensitivity to the $h \rightarrow \gamma\gamma$ signal hypothesis. The 95% confidence level limits on cross section multiplied by branching fraction relative to the SM prediction are summarized in Table IV and shown in Figure 4.

The invariant mass distribution of the two photons with data, background, and signal shapes for each mass point are shown in Figure 5, where the signal shapes are shown scaled

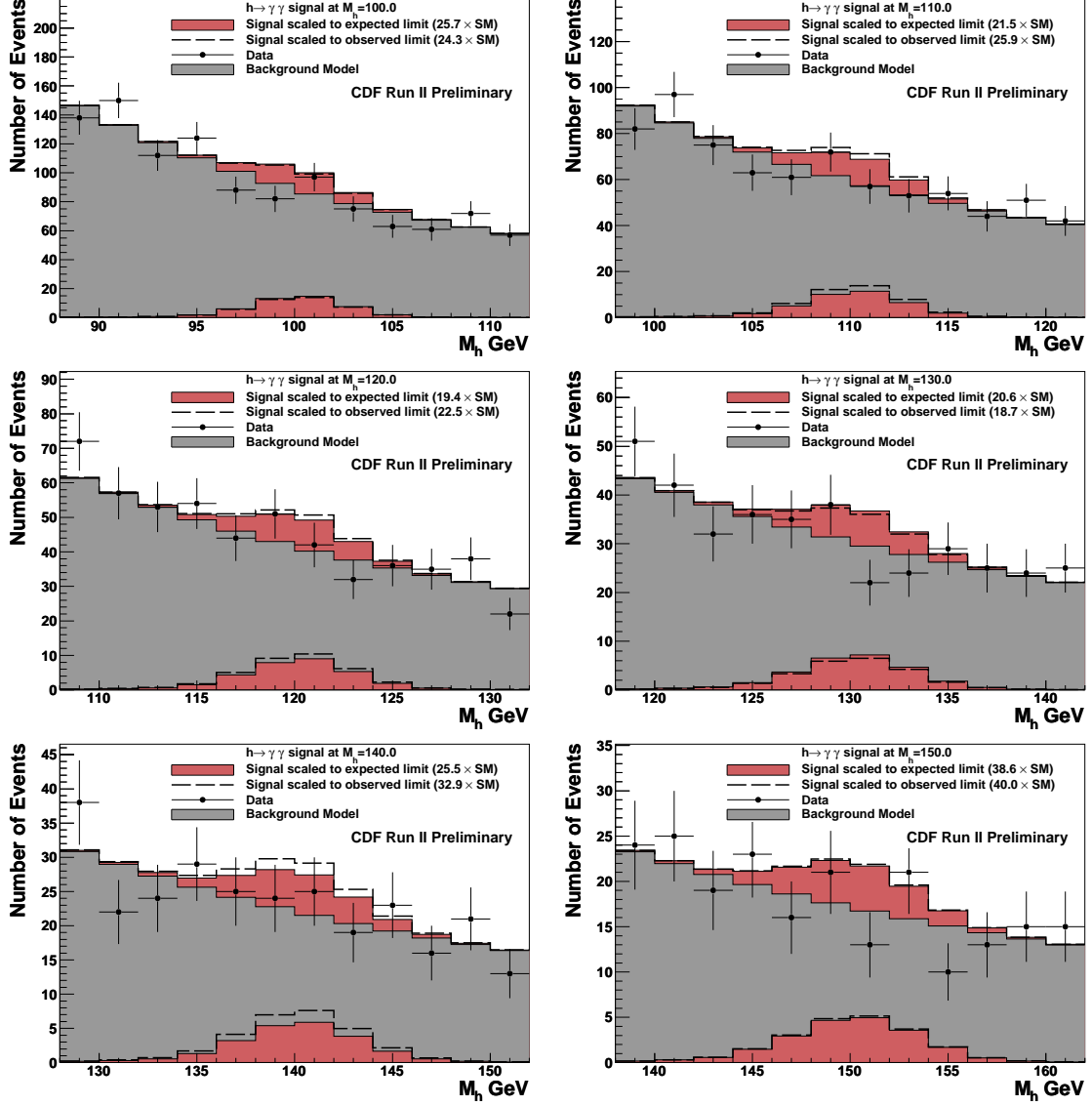


FIG. 5: Invariant mass distribution near each theoretical Higgs mass.

to the expected and observed limits found for that mass point.

VIII. CONCLUSIONS

A simple analysis was discussed which searched for $h \rightarrow \gamma\gamma$ in 5.4 fb^{-1} of CDF data in the central region of the detector. No significant excess over the background was observed, so we presented 95% C.L. upper limits on the production cross sections times branching fraction relative to the SM expectation. For Higgs masses between 100 and 150 GeV these limits range from 19.4 to 38.6.

Acknowledgments

We thank the Fermilab staff and the technical staffs of the participating institutions for their vital contributions. This work was supported by the U.S. Department of Energy and National Science Foundation; the Italian Istituto Nazionale di Fisica Nucleare; the Ministry of Education, Culture, Sports, Science and Technology of Japan; the Natural Sciences and Engineering Research Council of Canada; the National Science Council of the Republic of China; the Swiss National Science Foundation; the A.P. Sloan Foundation; the Bundesministerium fuer Bildung und Forschung, Germany; the Korean Science and Engineering Foundation and the Korean Research Foundation; the Particle Physics and Astronomy Research Council and the Royal Society, UK; the Russian Foundation for Basic Research; the Comision Interministerial de Ciencia y Tecnologia, Spain; and in part by the European Community's Human Potential Programme under contract HPRN-CT-20002, and the Academy of Finland.

-
- [1] S. Mrenna and J. D. Wells, Phys. Rev. **D63**, 015006 (2001), hep-ph/0001226.
 - [2] G. L. Landsberg and K. T. Matchev, Phys. Rev. **D62**, 035004 (2000), hep-ex/0001007.
 - [3] L. Authors (LEP Higgs Working Group) (2001), hep-ex/0107035.
 - [4] A. A. Affolder et al. (CDF), Phys. Rev. **D64**, 092002 (2001), hep-ex/0105066.
 - [5] V. Abazov et al. (D0) (2008), arXiv:0803.1514 [hep-ex].
 - [6] T. Aaltonen et al. (CDF), Phys. Rev. Lett. **103**, 061803 (2009), 0905.0413.
 - [7] V. Abazov et al. (D0), Phys. Rev. Lett. **102**, 231801 (2009).
 - [8] M. Spira (1998), hep-ph/9810289.
 - [9] T. Sjostrand et al., Comput. Phys. Commun. **135**, 238 (2001), hep-ph/0010017.
 - [10] H. L. Lai et al. (CTEQ), Eur. Phys. J. **C12**, 375 (2000), hep-ph/9903282.
 - [11] R. Field and R. C. Group (CDF) (2005), hep-ph/0510198.
 - [12] T. Aaltonen et al. (CDF) (2007), arXiv:0707.2294 [hep-ex].
 - [13] F. Abe et al. (CDF), Nucl. Instr. Meth. **A271**, 387 (1988).
 - [14] P. T. Lukens (CDF IIb) (2003), FERMILAB-TM-2198.
 - [15] R. Brun, F. Bruyant, M. Maire, A. C. McPherson, and P. Zanarini (1987),

CERN-DD/EE/84-1.

- [16] G. Grindhammer, M. Rudowicz, and S. Peters, Nucl. Instrum. Meth. **A290**, 469 (1990).
- [17] D. Stump et al., JHEP **10**, 046 (2003), hep-ph/0303013.
- [18] J. Pumplin et al., Phys. Rev. **D65**, 014013 (2002), hep-ph/0101032.
- [19] P. M. Nadolsky and Z. Sullivan, eConf **C010630**, P510 (2001), hep-ph/0110378.
- [20] D. Bourilkov, R. C. Group, and M. R. Whalley (2006), hep-ph/0605240.